Cement and Concrete Composites 74 (2016) 136–146

Contents lists available at ScienceDirect

Cement and Concrete Composites

journal homepage: www.elsevier.com/locate/cemconcomp

Electrochemical chloride removal for reinforced concrete with steel rebar cage using auxiliary electrodes

W. Yeih [a], J.J. Chang [a, *], C.C. Chang [a], K.L. Chen [a], M.C. Chi [b]

[a] Department of Harbor and River Engineering, National Taiwan Ocean University, Keelung, 202, Taiwan
[b] Department of Fire Science, WuFeng University, Chiayi County, 621, Taiwan

ARTICLE INFO

Article history:
Received 20 January 2016
Received in revised form
18 July 2016
Accepted 9 August 2016
Available online 12 August 2016

Keywords:
Electrochemical chloride removal
Steel rebar cage
Auxiliary electrodes
Corrosion

ABSTRACT

In this paper, a new approach of electrochemical chloride removal (ECR) using the auxiliary electrodes was proposed and the performances of this method were investigated by experiments. Two kinds of electrode setups were investigated: the radial type and the layer type. The results showed no matter which setup was used the chloride removal percentage all exceeded 70% after 8-week treatment. The chloride enclosed by the steel rebar cage could be successfully pushed out from concrete using auxiliary electrodes. The half cell potentials of rebars after 8-week treatment were all higher than −270 mV(CSE) and the corrosion rates were lower than 0.05 mpy, it indicated that after ECR treatment the corrosion risk of rebars was low. In addition, after ECR the surface hardness was enhanced via the results of rebound strength test. The pH value of concrete was also enhanced during the ECR process.

1. Introduction

Chloride attack is one major concern for concrete deterioration, and an over review article about the durability of concrete can be found in Ref. [1]. To deal with the concrete contaminated by chloride, removing unsound concrete and recasting repair material is one alternative and adopting ECR is another. Assessments and guidelines for ECR treatment were issued following the Strategic Highways Research Program (SHRP in the USA)—such as SHRP-S-347 and SHRP-C-620, which can be downloaded from the web. In addition, the processes were the subject of several patents which formed the basis of the “Norcure” processes that have been fairly widely known and used in USA, Europe and Japan. The idea of ECR involves mounting an anode surrounded by a liquid electrolyte (usually NaOH or Na_3BO_3) on the surface of concrete and driving direct current into the embedded reinforcement, which acts as a cathode. The current pushes chloride ions away from the reinforcement and extracts them towards the anode which is attached to concrete surface. Once reaching the concrete surface, the ions move into the anolyte and are thereby removed from concrete.

Liu et al. [2] proposed a three-phase model, which considers the multi-species coupling in pore solution, electrochemical reactions taking place at electrodes, multi-species binding between solid and liquid phases, as well as the effect of applied current density and treatment time, to investigate the efficiency of ECR. Li and Page [3] adopted the finite element to simulate ECR process, in which the effects of externally applied current density, treatment period, diffusion coefficients of concrete, ionic binding, boundary conditions and medium porosity on the efficiency of chloride extraction were studied. Wang et al. [4] used a two-dimensional model to study ECR process, and in this model the effects of electrostatic coupling of charged ions in a multi-component mixture and the influence of a number of other factors were considered. Toumi et al. [5] adopted Nernst-Planck model and numerically calculated the chloride profile in ECR process. Castellote et al. [6] calculated the chloride profile during ECR process by numerical model, and the decrease of the chloride diffusion coefficient of concrete due to the formation of hydroxyl ion concentration was taken into consideration using an empirical formula. Elsener and Angst [7] studied the mechanism of ECR. Due to the removal of free chloride during ECR, bound chloride is dissolved in order to re-establish the equilibrium between bound and free chlorides. The rate of release of bound chloride is slow compared to the rate of chloride removal, and thus ECR process quickly becomes inefficient. Current off periods allow the system to re-establish the equilibrium between bound and free chlorides, and consequently the ECR can become efficient again.

Fajardo et al. [8] studied the chloride removal efficiency of ECR and it was reported that about 60% to 50% of the initial chloride was

---

* Corresponding author.
E-mail address: jjc@ntou.edu.tw (J.J. Chang).

http://dx.doi.org/10.1016/j.cemconcomp.2016.08.002
0958-9465/© 2016 Published by Elsevier Ltd.

removed from the concrete on average using a current density of 1 A/m^2. Orellan et al. [9] investigated the removal efficiency and side effect of ECR. It was reported about 40% of the initial chloride content was removed from the steel rebar after 7-w treatment. However, microstructural observations by scanning electron microscopy (SEM) showed that after treatment new cementitious phases containing higher concentrations of sodium, aluminum and potassium were formed, which implied that the ECR might result in the alkali-silica reaction. Yeih et al. [10] investigated the relation between the polarization parameter (defined as the desalination current density times the duration of ECR) and the ECR efficiency. They concluded that as this parameter increased the chloride ion content inside concrete decreased.

Pérez et al. [11] adopted a conductive cement paste for ECR and the thickness of the conductive cement paste anode was found to have a great influence on the capacity of the anode to retain an important part of the extracted chlorides after finishing the ECR. Cañón et al. [12] investigated the feasibility of ECR using a spray conductive graphite powder-cement paste as anode, it was concluded that this kind of anode not only provided ECR with similar efficiency, but also retained moisture even without use of a continuous dampening system.

Miranda et al. [13] reported that if ECR is applied preventively it is an efficient procedure for retarding the start of corrosion. However, if applied too late it then does not assure the repassivation of corroded reinforcements and is therefore useless. Sánchez and Alonso [14] simultaneously adopted the ECR and corrosion inhibitor, and they confirmed the efficiency of the treatment by the visual inspection of the rebar as well as the analysis of chloride and nitrite around the rebar. Buenfeld and Broomfield [15] examined the bond status between rebar and concrete after ECR. Siegwart et al. [16] studied the effect of ECR on pre-stressed concrete, and they gave a warning that the risk of hydrogen induced brittle fracture due to electrochemical chloride extraction cannot be altered with modification of the treatment parameters, such as current density or treatment duration. According to their study, ECR should not be applied on pre-stressed concrete. Swamy and McHugh [17] investigated the effectiveness of ECR when applied to reinforced beams containing chlorides as well as chlorides and reactive aggregates.

The short and long-term efficiencies of ECR treatment on corrosion rate of corroded reinforcements were examined by Abdelaziz et al. [18]. The influences of water-cement ratio and cover thickness on ECR were investigated by Monteiro et al. [19]. Wang et al. [20] studied the change of properties for concrete after ECR. Their results showed that when ECR treatment was removed, the half cell potential tended to a more active state and corrosion rate became larger in comparison to those before ECR, then the half cell potential shifts to nobler potential and corrosion current decreased as time increased.

The degradation of bond between steel bar and freeze-thaw concrete was observed after ECR [21]. Gao and Yang [22] investigated the electrochemical changes of pre-corroded steel reinforced concrete after applying ECR. Their results showed that a higher water-cement ratio or more amount of fly ash was added eventually resulted in a severer corrosion happening on the reinforcing steel rebar prior to ECR treatment. Although the resistivity of cover concrete is remarkably improved, the corrosion state is aggravated after ECR treatment via studying the corrosion potential and corrosion current density evolutions. Ismail and Muhammad [23] investigated the ECR effect on reinforced concrete made with blended cements. They reported that chloride removal was more effective in ordinary Portland cement (OPC) in comparison with blended cements.

Garcés et al. [24] investigated the effects of bar arrangements on the ECR efficiency. Five different types of bar arrangements were studied, corresponding to typical structural members such as columns (with single and double bar reinforcing), slabs, beams and footings. They concluded that the ECR efficiency was influenced by the type of bar arrangement and a uniform layer set-up favors chloride extraction.

The conventional ECR process adopts the embedded steel as cathode. In our previous research [25], we reported that the chloride content enclosed by the steel cage was difficult to be removed by ECR efficiently. It means the conventional ECR can only effectively remove chloride ions of cover concrete. Some previous researches [26–28] reported that it is possible to extract significant amounts of chloride ions from regions behind the steel reinforcement levels, i.e. inside the steel rebar cage. However, it probably requires the passing of a high amount of electric charge through the ECR setup and a longer desalination time. Ihekwaba et al. [29] have reported the accumulation of chlorides in some regions inside the steel rebar cage. If the chloride contamination exists all over the reinforced concrete structure, how to remove them efficiently becomes an important task.

In this study, a novel ECR process was proposed. The graphite rods were embedded in concrete to play as auxiliary electrodes. Two types of electrode arrangement were evaluated: the first one is called the radial type and the second one is called the layer type. The chloride removal percentage of this proposed method was verified through chloride content profile. In addition, the pH value profile, rebound strength, half-cell potential and corrosion rate were measured to investigate the changes in properties of concrete after this proposed method.

2. Experimentation

2.1. Materials and specimen preparation

The concrete mix design is listed in Table 1. Type I cement is used; the fine aggregate is river sand from local source and the properties are: fineness modulus is 2.65, SSD specific weight is 2.66, water absorption is 2.98% and the sieve analysis is tabulated in Table 2. The coarse aggregate used is crushed stone and the properties are: fineness modulus is 6.36, SSD specific weight is 2.67, water absorption is 0.93%, the oven dry density is 1683 kg/m^3 and the sieve analysis is listed in Table 3. The #4 rebars are used as the major reinforcements and #3 rebars are used as the stirrups for specimens. The geometrical diagrams for rebars are depicted in Fig. 1 and the parameters are tabulated in Table 4. To simulate the contaminated concrete, a 3% cement weight dosage of NaCl is added in the concrete. The specimen has a size of 15 cm × 15 cm × 30 cm with four #4 rebars as major reinforcements and #3 rebars are used as stirrups, the lap distance of stirrups is 6 cm and the cover thickness is 2 cm. The diagram of specimens with rebar cage is shown in Fig. 2. Nine graphite rods (diameter of 1.0 cm) are embedded in the concrete to play as the auxiliary electrodes, and the properties of the graphite rod are tabulated in Table 5.

The specimens were cast and demolded after 24 h (1 day) and then kept in saturated lime water curing environment for 27 days. After that, the age of concrete reached 28-days. To conduct the ECR, the electrolyte solution used for anode cell was 0.1 M NaOH solution and for the group using cathode (for layer type electrode setup, which will be explained later) the electrolyte used for the cathode cell was tap water. The external electrodes in anode cell and cathode cell were platinized titanium meshes. The acrylic sheets were used to construct the anode cell and cathode cell, which contained different solutions. For more details, please refer to Fig. 3.

The ECR lasted for 8 weeks and for the ECR periods of 2, 4, 6 and 8 weeks various tests in section 2.2 were carried out.

Table 1
Concrete mix design.

W/c	Water (kg/m^3)	Cement (kg/m^3)	Fine aggregate (kg/m^3)	Coarse aggregate (kg/m^3)	NaCl (kg/m^3)
0.5	196	393	662	1046	11.79

Table 2
Sieve analysis of fine aggregates.

Sieve number (ASTM)	Retained mass (kg)	Percent retained (%)	Cumulative % retained
#4	0	0	0
#8	0.02	2	2
#16	0.075	7.5	9.5
#30	0.285	28.5	38
#50	0.475	47.5	85.5
#100	0.125	12.5	98
Pan	0.02	2	

F. M. = 2.33.

Table 3
Sieve analysis of coarse aggregates.

Sieve number (ASTM)	Retained mass (kg)	Percent retained (%)	Cumulative % retained
1″	0	0	0
3/4″	0.46	4.6	4.6
1/2″	2.925	29.25	33.85
3/8″	1.605	16.05	49.9
#4	4.310	43.1	93
Pan	0.7	7	

F. M. = 6.48.
Maximum aggregate size = 19 mm.

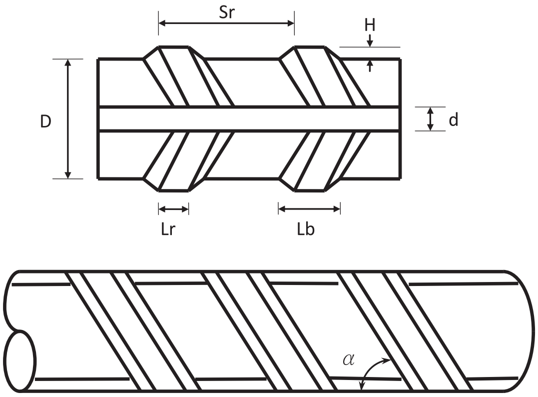

Fig. 1. Geometric diagrams of rebar.

Electrochemical corrosion signal measurements were performed after 1-w depolarization time to avoid misreading the meanings.

The setup for ECR process is illustrated in Fig. 3. For setup A, it is named as the radial type setup. The potential of the anode surrounding concrete is highest, and the potential of the central graphite rod is lowest. The potential of other eight graphite rods is medium. Consequently, it is expected the electric current will flow from surrounding anode to the eight graphite rods and finally to the central graphite rod. The potential difference between the anode and the 8 graphite rods is 10 V. The potential difference between the 8 graphite rods and the central graphite rod is 10 V also. It is noticed that for the 8 graphite rods, they play as the anode and cathode at the same time in different cells. Therefore, it is important that the auxiliary electrodes should be conductive but noble material to prevent possible corrosion takes place. In a preliminary study, we have tried 304 stainless steels to play as the auxiliary electrodes. However, liquid containing rust leached out very soon.

For setup B, it is named as the layer type setup. The cathode is placed on the top of concrete and the anode is placed on the bottom of concrete. We have three layers of graphite rods (each layer has three graphite rods) and the potentials of graphite rods for each layer are the same. The potential difference between anode and the third layer is 5 V, the potential difference between two adjacent layers is 5 V, and the potential difference between the first layer and cathode is 5 V also. For both setups, the potential differences between anode and cathode are 20 V. The constant voltage of 20 V is adopted according to our previous study [30]. When potentiostatic condition is used, the electric current density decreases as the desalination time continues since the electric resistance of concrete increases due to the formation of calcium deposit and the electrolysis of water near electrodes (depending on the electrochemical reactions of the anode and cathode). On the other hand, when the constant current density condition is adopted the potential difference between electrodes increases as desalination time increases

Table 4
Geometric parameters for rebars.

Steel no.	Area (cm^2)	D (mm)	d (mm)	Lr (mm)	Lb (mm)	H (mm)	α (degree)	Sr (mm)
NO.3	0.71	9.52	2.96	0.86	1.54	0.54	66	6.24
NO.4	1.29	12.30	3.99	1.36	2.24	0.74	66	8.23

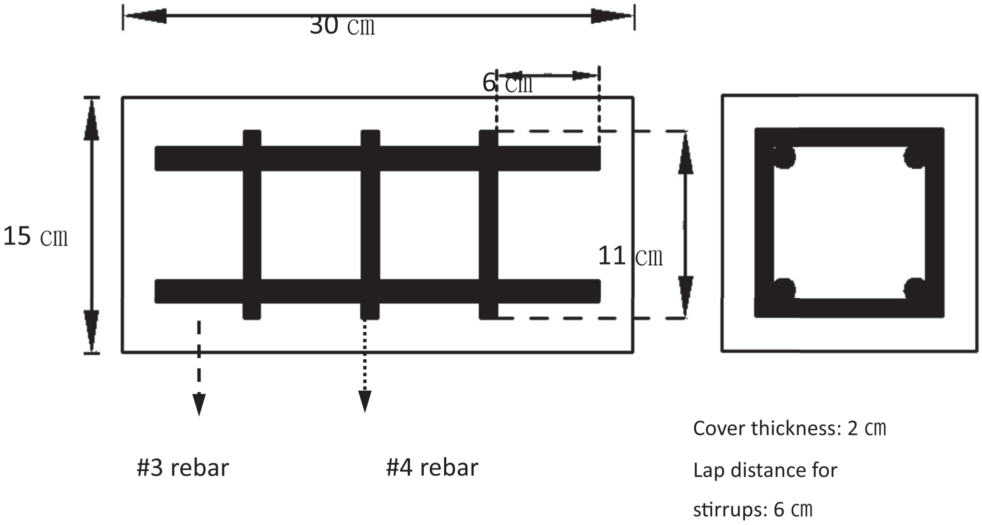

Fig. 2. Specimens with steel reinforcement cage.

Table 5
Properties of graphite rod.

Density (g/cm^3)	Resistance (μΩcm)	Bending strength (MPa)	Compressive strength (MPa)	Hardness (Hs)	Thermal expansion coeff. (10^{-6}/°C)
1.80	1250	45	95	64	4.6

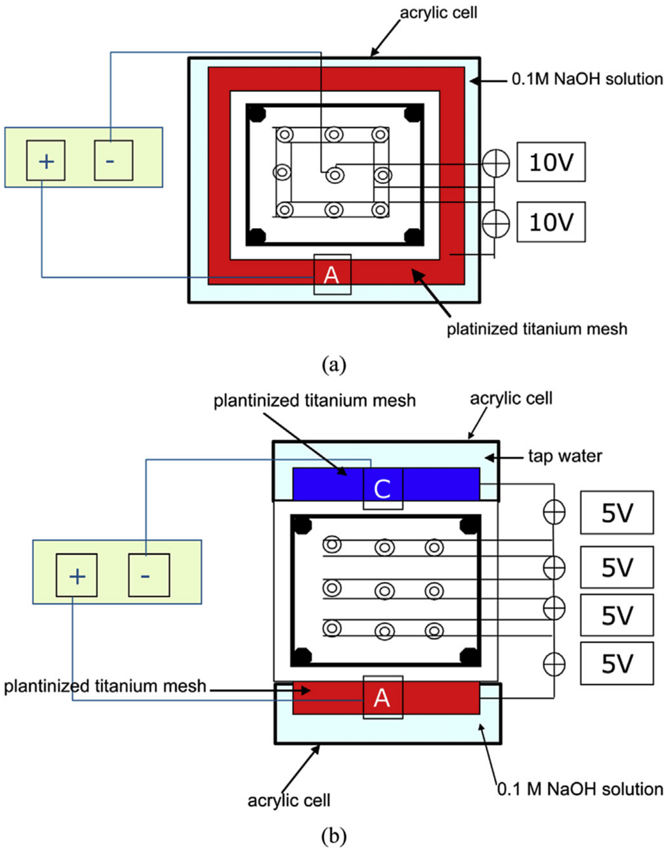

(a)

(b)

Fig. 3. Electrode setups: (a) setup A-radial type; (b) setup B-layer type.

due to increase of the electric resistance of concrete. Although many previous researches adopted the constant current density condition and reported suggested current density level for desalination, it is difficult to compare our results to these reports as explained in the above. Therefore, in this study we only compare results with our previous research [25] which adopted the potentiostatic condition.

2.2. Experiments conducted

2.2.1. Rebound strength

The rebound strength although is not reliable (the rebound strength result may be affected by many factors such as the water content in concrete, impact angle of rebound hammer and others. Therefore, it can be referred as a reference but not a reliable test.) yet can provide a non-destructive test for evaluating the concrete surface soundness as well as the compressive strength. Since the specimens contained reinforcement cage such that the compressive strengths of the specimens cannot be measured. Instead of using take-core compressive strengths, the rebound strengths were used to represent the mechanical properties of concrete. When each ECR period was reached, the rebound strength tests were performed for 10 marked points as shown in Fig. 4 (red x marks). These marked points are at the centers for selected square region. The estimated concrete compressive strength then was obtained using the average of these data. In Ref. [31], the procedures for performing the rebound strength can be found.

2.2.2. Chloride content

The sampling method is first introduced in the followings. A 3-cm width slab was cut from the specimen as shown in Fig. 4 and 25 sampling points (each sampling point locates at the center of the selected square region) were taken as shown in Fig. 4. The chemical titration was then carried out to determine the water soluble chloride content inside the concrete. Using these 25 data for a specific ECR period, one can construct the chloride ion concentration contours and to check the efficiency of ECR. The contours are

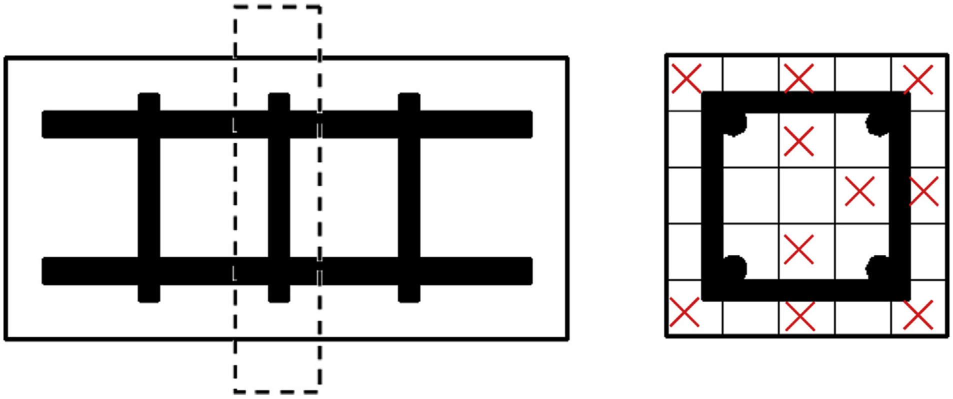

Fig. 4. Sampling methods for steel reinforcement cage specimen. (X: locations for rebound strength tests).

generated using the radial basis function approximation. The standard for measuring water soluble chloride ions can refer to ASTM C1218/C1218M-99. Usually the water soluble chloride content is referred to the free chloride ions which affect the corrosion of reinforcement. When the desalination process takes place, the value of water soluble chloride ion may come from two folds: the original free chlorides and some chloride ions which are originally bound chlorides (they become free chlorides because of the equilibrium between bound and free chlorides).

2.2.3. pH values

It is known that the cathodic current will generate hydroxide ions near cathode and thus the pH value will be increased. The sampling method for measuring pH value is the same as the chloride content experiment. A 3-gram grounded sample which passed #50 sieve was prepared for each sampling point and it then was added into a 50 ml distilled water and this solution was heated for 5 min. The container of the solution then was sealed by PVC film in order to avoid contamination and vaporization and it was placed for 24 h. The solution was then heated again for 15 min; the solution passing through the filter paper was collected. The solution was diluted into 1000 ml solution; the hydroxide ion concentration was determined by chemical titration method. Using this, the relative pH value for the original sample was obtained. It is worth mentioned here that the pH value here is not the pH value of the pore solution. The pH value we obtain here can be understood as the alkalinity the concrete may provide after ECR. If this value is low, it implies that the pH value of pore solution may be also low.

2.2.4. Half cell potential

The half cell potential can provide thermodynamic trend for the rebar corrosion. The ASTM C876 provides a guide for conducting the half cell test. When each ECR period was fulfilled, the specimens then were disconnected first and 1-w depolarization time was required before measurement. Usually immediately after the disconnection of electric current, the half cell potential tends to a very active potential, which may lead us to make a judgment that the rebar suffers from corrosion. In order to avoid this, a sufficiently long time is necessary before the measurement. Actually, the half cell potentials measured immediately after disconnection were in the region for −950 mV ~ −1120 mV (CSE).

2.2.5. Instantaneous corrosion rate

The instantaneous corrosion rate was measured using the apparatus GPM-5000 manufactured by Germann Instruments. The GPM-5000 first measured the open circuit potential for the rebar. A pulse of current of this corrosion potential (usually 5–40 mA) was released for 10 s (suggested instrumental setup), the current was then cut off. After cutoff, the measurement of potential change could be carried out as shown in Fig. 5. Using these data, the instantaneous corrosion rate could be obtained. For details, please refer to [25].

Once again, since this method needs to know the half cell potential first the depolarization time is then necessary for accurate and meaningful measurements. According to the suggestions from the manufacturer, the relations between the corrosion current density and corrosion status are tabulated in Table 6.

2.2.6. Four-probe resistivity measurement

Wenner four-probe resistivity was conducted to check the resistivity change after ECR treatment. According to [32], the value of resistivity may be affected by the steel cage since the cover thickness is only 2-cm. However, once the condition kept the same, the resistivity values after ECR can be regarded as a comparative index.

3. Results and discussion

3.1. Rebound strength

The results of rebound strengths for specimens after ECR are depicted in Fig. 6. The initial 28-d bound strength was 26 MPa. It can be seen as the ECR process continued, the rebound strength increased. The rebound strength gain for setup A was lower than setup B for the same desalination time. If the initial 28-d bound strength is assumed to be 100%, the compressive strength gains for two setups are depicted in Fig. 7. It can be found after 8-w ECR

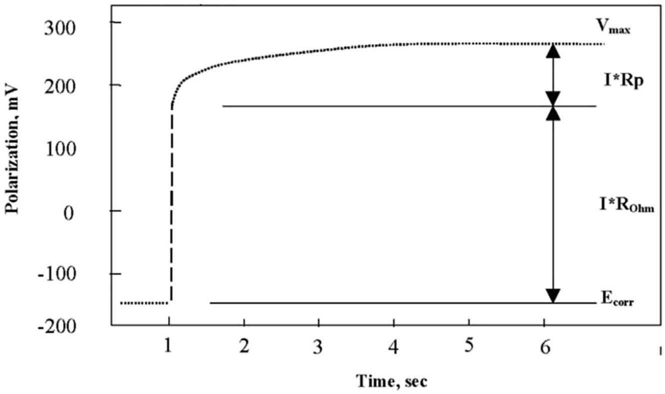

Fig. 5. A typical diagram for andic polarization after the cutoff of current for GPM.

Table 6
Relation between corrosion current density and corrosion status (suggested by manufacturer).

Corrosion current density (μA/cm^2)	Corrosion rate (mpy)	Corrosion status
<0.5	<0.23	Ignore
1.5–5	0.23–2.3	Low
5–10	2.3–4.6	Medium
10–15	4.6–6.0	High
>15	>6.9	Heavy

treatment, the rebound strength for concrete using setup A reached 171.17% while the rebound strength for concrete using setup B reached 173.85%. It implied the surface hardness became larger after ECR process. According to our previous research [25], the rebound strength related to the area of cathode. It is known that during ECR, the calcium ions will be attracted by cathode and the calcium carbonate will be formed. Remember that graphite rod plays as anode and cathode at the same time in different cells. It is obviously that the total area of cathode for setup A is lower than that for setup B. Therefore, the rebound strength for setup B was higher than setup A. After 8-w ECR treatment the rebound strength for both setups reached more than 170% of the initial value, however, rebound strength only reflects the surface hardness and it does not imply the compressive strength for concrete after ECR treatment also increases so much.

3.2. Chloride content

Initially the water-soluble chloride ion content for 28-day is 7.053 (kg Cl^-/m^3 concrete). This value was determined using ASTM C1218/C1218M-99. From the mix design in Table 1, the initial total chloride content is 7.15 (kg Cl^-/m^3 concrete). The water-soluble chloride ion content is lower than the initial total chloride content since part of added chloride is chemically bounded.

The chloride removal percentage for a specific ECR treatment time is calculated by the following formula:

$$P_i(t) = \frac{(A - B_i(t))}{A} \times 100\% \tag{1}$$

where P_i is the chloride removal percentage for the i-th sampling region, A is the initial chloride ion content which is 7.053 (kg Cl^-/m^3 concrete) and B_i is the chloride ion content for the i-th sampling region.

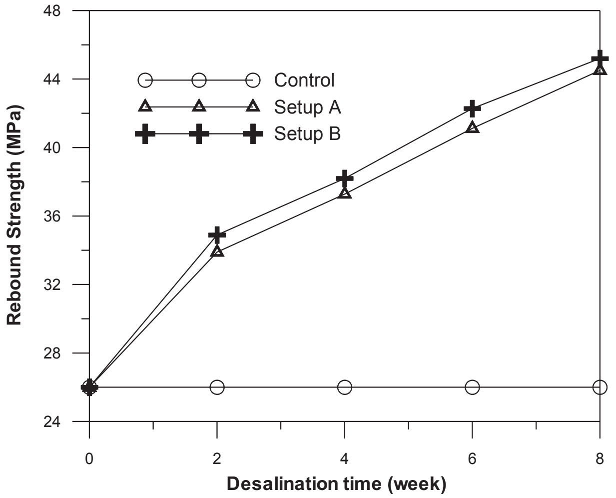

Fig. 6. Rebound strengths for ECR.

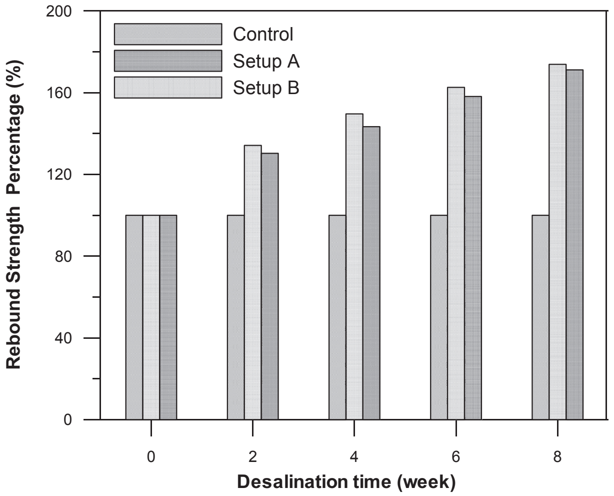

Fig. 7. Rebound strength percentage versus desalination time.

The total chloride removal percentage of ECR, E, is estimated by

$$E = \frac{\sum_{i=1}^{25} P_i}{25}. \tag{2}$$

In Eq. (2), the value of 25 in the denominator represents the number of sampling points.

The chloride removal percentages for two ECR setups are illustrated in Fig. 8. The chloride removal percentage increased as the desalination time increased. After 8-w ECR treatment, the chloride removal percentage of setup A reached 73% while the efficiency of setup B reached 78%. According to our previous research [25], the best chloride removal percentage for conventional ECR (steel cage plays as the cathode) could only reach 50% among many setups of electrodes. It means the current approach removes more chloride ions than the conventional one. In addition to that, the chloride removal percentage for setup B was a little bit better than setup A for any desalination time but the difference is not so significant.

The chloride distribution contours for setup A and setup B after 2, 4, 6 and 8-w ECR treatment are depicted in Figs. 9 and 10, respectively. Chloride ions decreased first from the center and then gradually the region of low chloride ion concentration expanded to

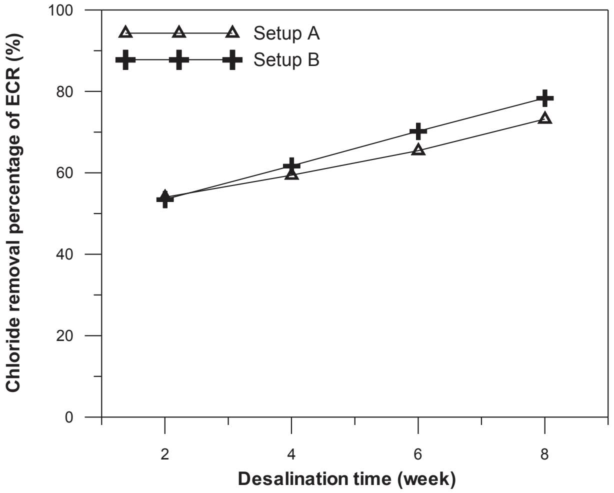

Fig. 8. Chloride removal percentages for two ECR setups.

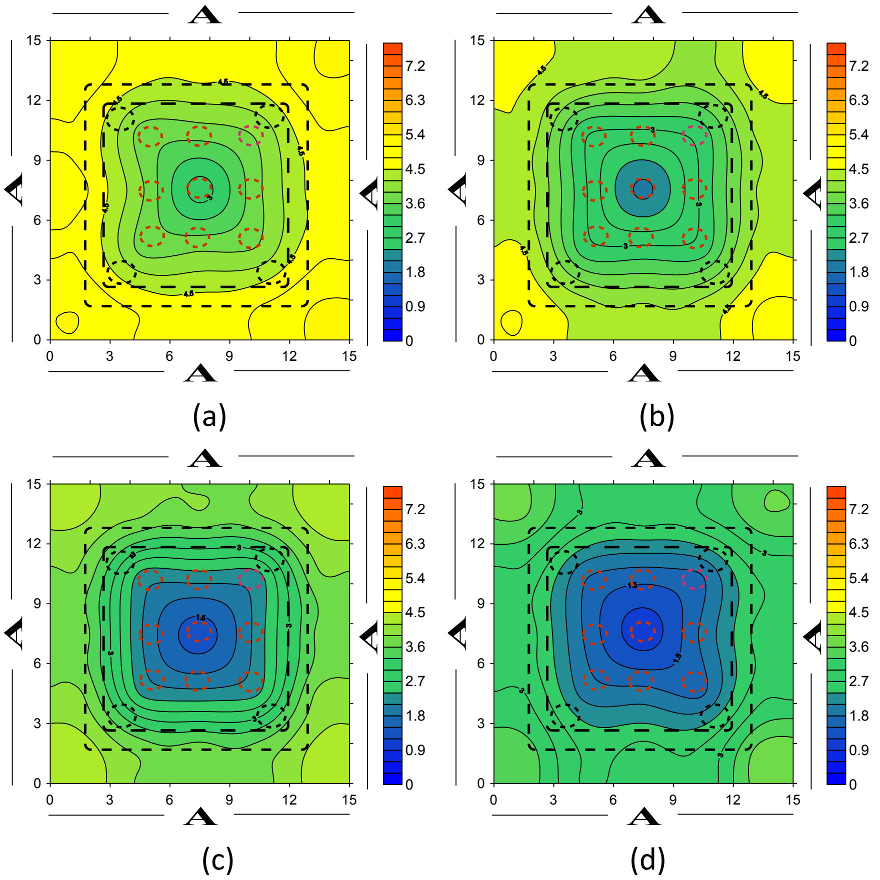

Fig. 9. The chloride ion distributions for ECR setup A for desalination time of: (a)2-w; (b) 4-w; (c) 6-w; (d)8-w. [Unit: kg(Cl^-)/m^3(concrete)].

outer region as time increased for ECR setup A. For setup B, the current starts from external anode (at the bottom of concrete surface) then passes through the lower layer of auxiliary electrodes, medium layer of auxiliary electrodes, upper layer of auxiliary electrodes and finally to the external cathode (at the top of concrete surface). Therefore, the decrease of chloride content starts from the lower part of the specimen (near the lower auxiliary electrodes) since the movement of chloride ions was in the backward direction of electric current. Chloride ions were pushed from external cathode to external anode gradually for setup B. These observations match physical intuition. In Ref. [25], the conventional ECR setup could not efficiently remove the chloride ions enclosed by the steel cage (Fig. 9 in Ref. [25]). For all ECR setups in Ref. [25], after 6-w ECR treatment, the chloride concentration inside the steel cage remained about 4–6 kg(Cl^-)/m^3(concrete). For our new proposed ECR setups using auxiliary electrodes, the chloride concentration inside the steel cage was about 0–3.6 kg(Cl^-)/m^3(concrete). It is obvious that the current approach successfully removes chloride ions enclosed inside the steel cage.

Here we want to make some comments on the terminology of “efficiency”. In previous researches, many researchers use this terminology without clear definition. For example in Ref. [2], the “efficiency” meant total removed chlorides divided by the constant current density applied (they applied the constant current density condition). In our previous research [25], the “efficiency” represented the total removed chloride percentage divided by the constant potential difference. A correct definition of “efficiency” might be defined as the total energy used for removing chlorides (which should have relation with total removed chloride percentage) divided by the total input electric energy.

In such definition, the total input electric energy needs to be measured no matter the constant current density condition or constant potential difference condition is used. Remember that as the desalination process continue, the resistivity of concrete changes such that one needs to measure the current density changes for the constant potential difference condition or the potential changes for the constant current density condition.

Therefore, when we mention that the chloride removal percentage of setup B is higher than that of setup A it does not imply that the efficiency of setup B is higher than that of setup A.

3.3. pH value

The pH value contours for setup A and setup B at different desalination times are illustrated in Figs. 11 and 12, respectively. For setup A, high pH value region started first from center and then expanded radially as time increased which matched our physical intuition. For setup B, high pH value region appeared first near cathode and then gradually expanded to the anode as time increased. Hydroxyl ions are formed near cathode for ECR setup and then as time increases they are pushed toward to the anode. Compare these two setups, pH value for setup B enhanced a little bit higher than setup A. The reason may come from the fact for setup B the area of cathode is higher than setup A.

In comparison with results in Ref. [25], setup B still cannot compete with setup C1 (Fig. 11 in Ref. [25]) in pH enhancement. For

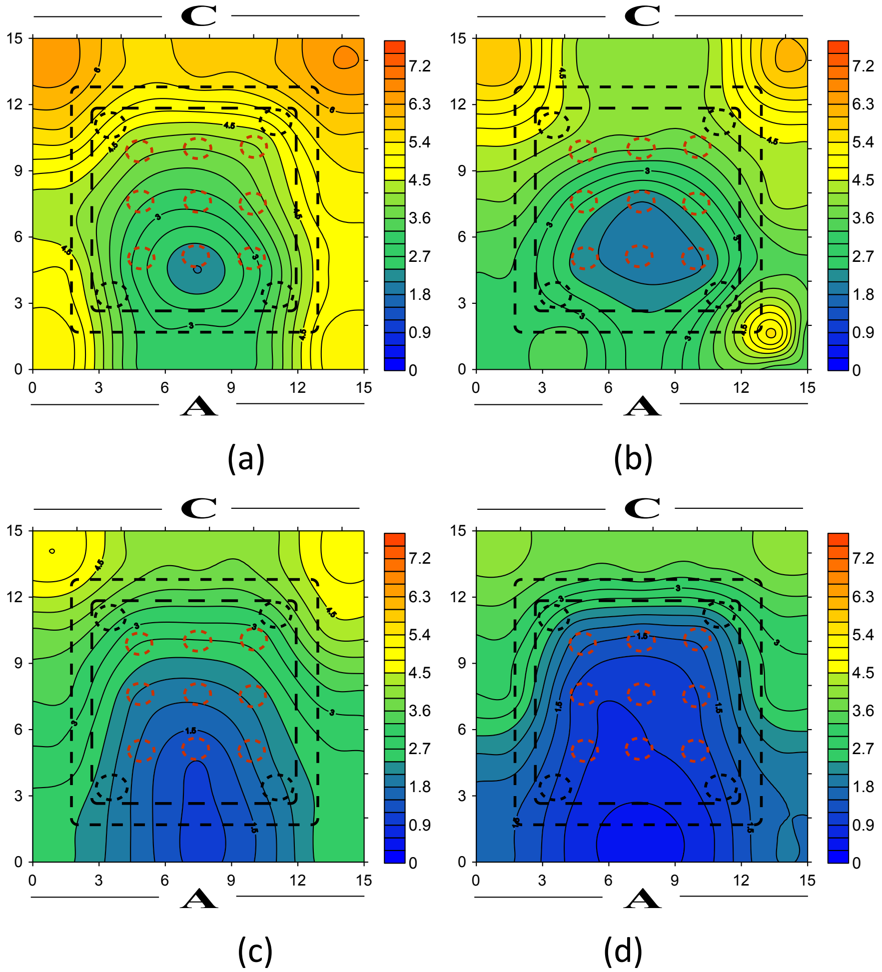

(a) (b) (c) (d)

Fig. 10. The chloride ion distributions for ECR setup B for desalination time of: (a)2-w; (b) 4-w; (c) 6-w; (d)8-w. [Unit: kg(Cl$^-$)/m^3(concrete)].

setup B in this article, the area of cathode contain the external cathode and all graphite rods; for setup C1 in Ref. [25] the area of cathode contain the external cathode and steel rebar cage. The area of steel rebar cage (including the major reinforcement and stirrups) is higher than that of graphite rods.

3.4. Half cell potential

The half cell potential indicates the thermodynamic trend for rebar corrosion. The half cell potentials and the instantaneous corrosion rates were measured using GPM apparatus. Before measurement, 1-w depolarization time was selected to avoid possible misleading judgment. For setup B, the chloride ions were pushed from cathode to anode. It is then expected that the corrosion status for rebar near cathode may be different from that for rebar near anode. For setup A, chloride ions were pushed from the central graphite rod to the anode and corrosion status for all rebars are expected the same. The half cell potential measurements are illustrated in Fig. 13. The initial half cell potentials for both setups were near −500 mV, CSE, which implied rebar is under high risk of corrosion. As desalination time increased, the half cell potential all tended to the nobler direction.

Compare the half cell potential for rebar near cathode and that near anode for setup B, it can be observed that the half cell potential for rebar near cathode was nobler than that near anode. This might come from the facts the chloride ion content near cathode is lower than that near anode and the pH value near cathode is higher than that near anode. When chloride content is lower and pH value is higher, the rebar pitting corrosion has lower chance to take place.

If we compare current results with that obtained in Ref. [25] (Fig. 12 in Ref. [25]), one can find that our current proposed setups all reached a nobler half cell potential than the conventional ECR setups.

3.5. Instantaneous corrosion rate

The half cell potential can only provide thermodynamic trends for rebar corrosion but it cannot really tell us how fast the rebar corrodes. To know how fast the rebar corrodes, the instantaneous corrosion rate is a better indicator. The corrosion rate measurements for both setups are depicted in Fig. 14. Before ECR treatment, the corrosion rate was about 8 mpy. According to Table 4, the corrosion status is heavy. After ECR treatment, the corrosion rate dropped dramatically. After 8-w ECR treatment, corrosion rate of rebar in setup A, that near cathode in setup B and that near anode in setup B were 0.01, 0.01 and 0.05 mpy, respectively. All these values indicated that the corrosion status became “ignore” after ECR treatment.

It is interesting to find that for setup B at different desalination

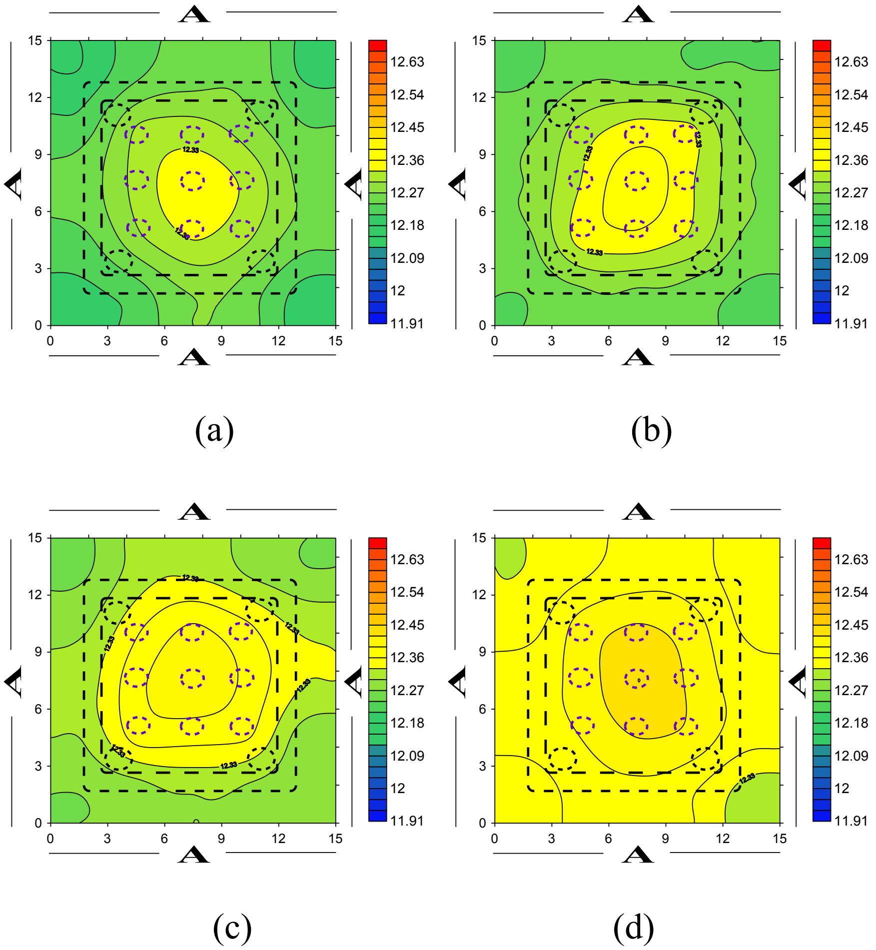

(a) (b)

(c) (d)

Fig. 11. The pH value for ECR setup A at desalination time: (a) 2-w; (b) 4-w; (c) 6-w; (d) 8-w.

times, the corrosion rate for rebar near cathode was always lower than that near anode. The reason has been provided in the explanation for phenomenon in half cell potential.

Comparing our results with those in Ref. [25] (see Fig. 13 in Ref. [25]), our proposed ECR setups helped embedded rebar to have a lower corrosion rate than the conventional ECR setups.

3.6. Four-probe resistivity measurement

The four probe resistivity measurements are depicted in Fig. 15. The initial resistivity before ECR treatment was 1.3 kΩ−cm. As the desalination time increased, the resistivity increased as well. This increasing resistivity may come from the formation of calcium carbonate which blocks the migration of ions. In addition, for the same desalination time the resistivity for concrete under ECR setup B was higher than setup A. The total area of cathode for setup B is larger than that for setup A. It is known that the calcium ions are attracted by cathode and formation of calcium carbonate takes place near cathode. Consequently, the setup having higher cathode area should have a higher resistivity value.

3.7. Some comments on the conventional ECR and the proposed ECR with auxiliary electrodes

According to our results, the proposed ECR with auxiliary electrodes can efficiently remove chlorides everywhere inside concrete. For conventional ECR, to remove chlorides inside the rebar cage although might be possible according to previous researches [26–28], however, it may require a higher amount of electric current. It needs to be mentioned here that the conventional ECR is a practically non-destructive rehabilitation technique, but this would not be the case if we need to embed the auxiliary electrodes inside the steel rebar cage before applying ECR. Obviously, a different situation would appear if the auxiliary electrodes were inserted before pouring the concrete into the forms, i.e. if installation of the auxiliary electrodes were considered at the design phase of the structure.

As mentioned earlier, we do not compare the “efficiency” of the proposed ECR setup and only compare the chloride removal percentages from our proposed ECR setup with those in Ref. [25]. To really understand the “efficiency” of an ECR setup, one should understand the work done for removing chlorides and the input electric energy. Only under this definition, one can compare results from different ECR setups no matter what condition is used (constant current density or constant potential difference).

4. Conclusion

In this article, the graphite rods are used to play as the auxiliary electrodes in ECR setups. The chloride removal percentage for the layer type setup (setup B) is better than the radial type setup (setup A) although the difference is not so significant. In addition,

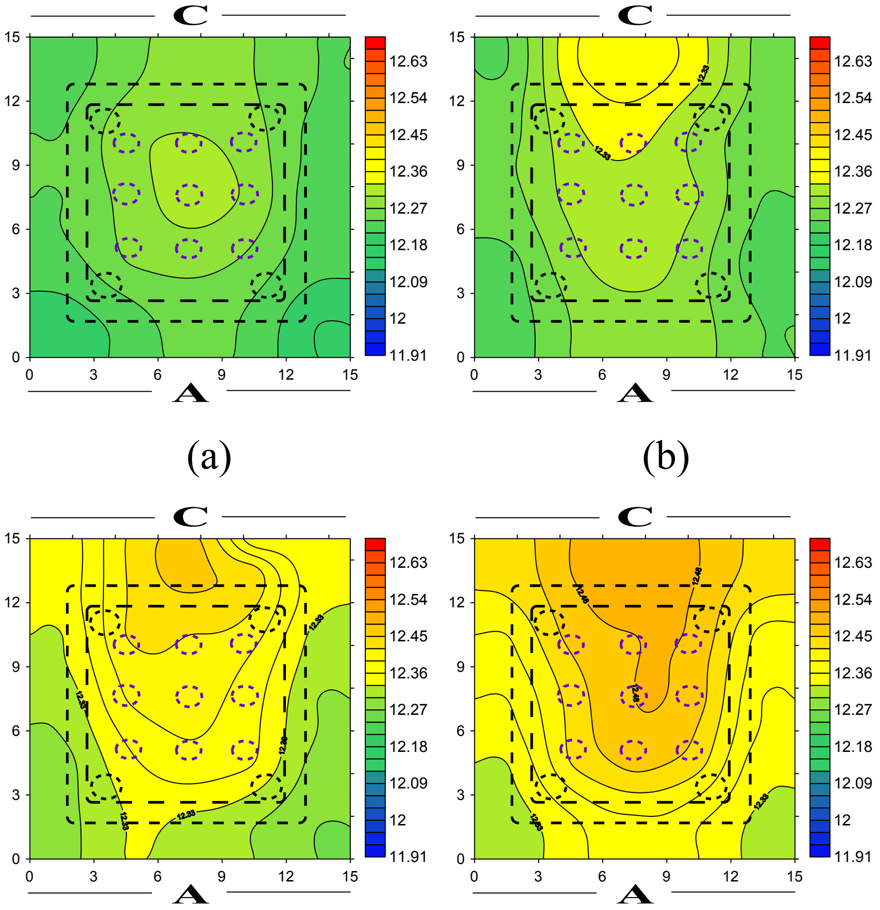

(a)

(b)

(c)

(d)

Fig. 12. The pH value for ECR setup B at desalination time: (a) 2-w; (b) 4-w; (c) 6-w; (d) 8-w.

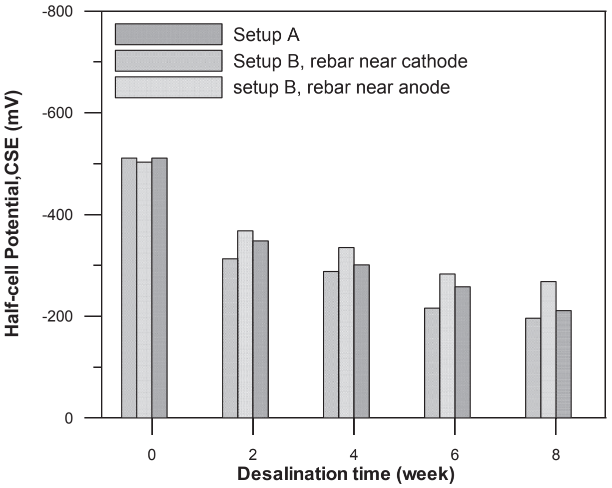

Fig. 13. Half cell potentials for different ECR setups.

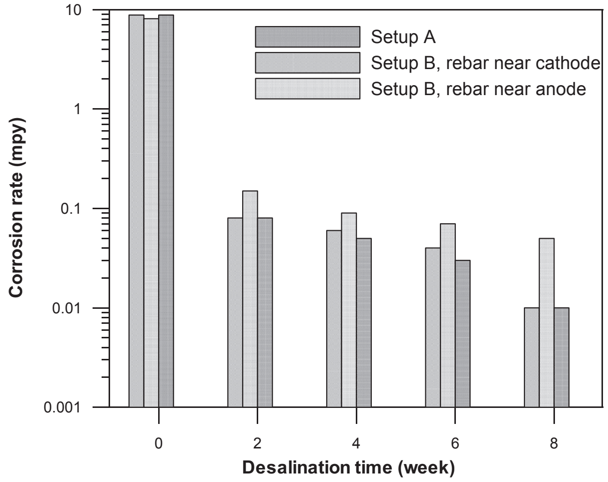

Fig. 14. Corrosion rates for different ECR setups.

the current ECR setups perform much better than the conventional ECR setups by comparing their chloride removal percentages. The pH value enhancement takes place around cathode and expanded to the anode gradually. The half cell potential and corrosion rate for the current ECR setups all show a more satisfactory value than those for the conventional ECR setups. In addition, the electrochemical signals show the corrosion risk for rebar near cathode is lower than that for rebar near anode. The resistivity of concrete in the layer type ECR setup becomes higher than that in the radial type ECR setup. The ECR setup with

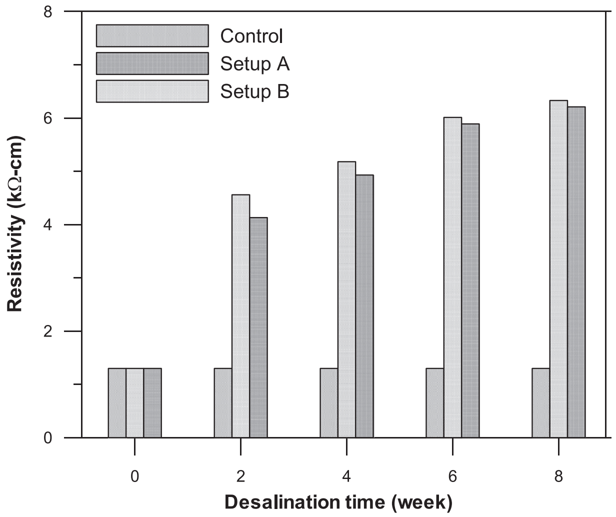

Fig. 15. Four-probe resistivity values for different ECR setups.

auxiliary electrodes can successfully remove the chloride inside the steel cage.

Acknowledgment

The authors would like to express his thanks for the financial support from the National Science Council, Taiwan under the grant number NSC 99-2221-E-019-033-MY3.

References

[1] X. Shi, N. Xie, K. Fortune, J. Gong, Durability of steel reinforced concrete in chloride environments: an overview, Constr. Build. Mater. 30 (5) (2012) 125–138.
[2] Q. Liu, J. Xia, D. Easterbrook, J. Yang, L. Li, Three-phase modelling of electrochemical chloride removal from corroded steel-reinforced concrete, Constr. Build. Mater. 70 (2014) 410–427.
[3] L.Y. Li, C.L. Page, Finite element modelling of chloride removal from concrete by an electrochemical method, Corros. Sci. 42 (12) (2000) 2145–2165.
[4] Y. Wang, L.Y. Li, C.L. Page, A two-dimensional model of electrochemical chloride removal from concrete, Comput. Mater. Sci. 20 (12) (2001) 196–212.
[5] A. Toumi, R. François, O. Alvarado, Experimental and numerical study of electrochemical chloride removal from brick and concrete specimens, Cem. Concr. Res. 37 (1) (2007) 54–62.
[6] M. Castellote, C. Andrade, C. Alonso, Electrochemical removal of chlorides: modelling of the extraction, resulting profiles and determination of the efficient time of treatment, Cem. Concr. Res. 30 (4) (2000) 615–621.
[7] B. Elsener, U. Angst, Mechanism of electrochemical chloride removal, Corros. Sci. 49 (12) (2007) 4504–4522.
[8] G. Fajardo, G. Escadeillas, G. Arliguie, Electrochemical chloride extraction (ECE) from steel-reinforced concrete specimens contaminated by artificial sea-water, Corros. Sci. 48 (1) (2006) 110–125.
[9] J.C. Orellan, G. Escadeillas, G. Arliguie, Electrochemical chloride extraction: efficiency and side effects, Cem. Concr. Res. 34 (2) (2004) 227–234.
[10] W. Yeih, J.J. Chang, C.C. Hung, Selecting an adequate procedure for the electrochemical chloride removal, Cem. Concr. Res. 36 (3) (2006) 562–570.
[11] A. Pérez, M.A. Climent, P. Garcés, Electrochemical extraction of chlorides from reinforced concrete using a conductive cement paste as the anode, Corros. Sci. 52 (5) (2010) 1576–1581.
[12] A. Cañón, P. Garcés, M.A. Climent, J. Carmona, E. Zornoza, Feasibility of electrochemical chloride extraction from structural reinforced concrete using a sprayed conductive graphite powder–cement paste as anode, Corros. Sci. 77 (2013) 128–134.
[13] J.M. Miranda, A. Cobo, E. Otero, J.A. González, Limitations and advantages of electrochemical chloride removal in corroded reinforced concrete structures, Cem. Concr. Res. 37 (4) (2007) 596–603.
[14] M. Sánchez, M.C. Alonso, Electrochemical chloride removal in reinforced concrete structures: improvement of effectiveness by simultaneous migration of calcium nitrite, Constr. Build. Mater. 25 (2) (2011) 873–878.
[15] N.R. Buenfeld, J.P. Broomfield, Influence of electrochemical chloride extraction on the bond between steel and concrete, Mag. Concr. Res. 52 (2) (2000) 79–91.
[16] M. Siegwart, J.F. Lyness, B.J. McFarland, G. Doyle, The effect of electrochemical chloride extraction on pre-stressed concrete, Constr. Build. Mater. 19 (8) (2005) 585–594.
[17] R.N. Swamy, S. McHugh, Effectiveness and structural implications of electrochemical chloride extraction from reinforced concrete beams, Cem. Concr. Compos 28 (8) (2006) 722–733.
[18] G.E. Abdelaziz, A.M.K. Abdelalim, Y.A. Fawzy, Evaluation of the short and long-term efficiencies of electro-chemical chloride extraction, Cem. Concr. Res. 39 (8) (2009) 727–732.
[19] P.J.M. Monteiro, P. Helene, I. Aoki, P. Barbosa, E. Monteiro, Influence of water-cement ratio and cover thickness on chloride extraction of reinforced concrete, ACI Mater. J. 102 (1) (2005) 9–14.
[20] X. Wang, Q. Yu, C. Deng, J. Wei, Z. Wen, Change of electrochemical property of reinforced concrete after electrochemical chloride extraction, J Wuhan U Tech. Mater. Sci. Ed 22 (4) (2007) 764–769.
[21] Y. Guo, J. Gong, Degradation of bond between steel bar and freeze-thaw concrete after electrochemical chloride extraction, J Cent. South U Tech. 17 (2) (2010) 388–393.
[22] X. Gao, Y. Yang, Electrochemical changes of pre-corroded steel reinforced concrete due to electrochemical chloride extraction, Int. J. Electrochem Sci. 6 (2011) 1797–1809.
[23] M. Ismail, B. Muhammad, Electrochemical chloride extraction effect on blended cements, Adv. Cem. Res. 23 (5) (2011) 241–248.
[24] P. Garcés, M.J. Sánchez de Rojas, M.A. Climent, Effect of the reinforcement bar arrangement on the efficiency of electrochemical chloride removal technique applied to reinforced concrete structures, Corros. Sci. 48 (3) (2006) 531–545.
[25] C.C. Chang, W. Yeih, J.J. Chang, R. Huang, Effects of stirrups on electrochemical chloride removal efficiency, Constr. Build. Mater. 68 (2014) 692–700.
[26] I.L.H. Hansson, C.M. Hansson, Electrochemical extraction of chlorides from concrete. Part I- A qualitative model of the process, Cem. Concr. Res. 23 (1993) 1141–1152.
[27] B.B. Hope, N.M. Ihekwaba, C.M. Hansson, Influence of multiple rebar mats on electrochemical removal of chloride ions from concrete, Mater. Sci. Forum 192–194 (1995) 883–890.
[28] M.A. Climent, M.J. Sanchez de Rojas, G. de Vera, P. Garces, Effect of type of anodic arrangements on efficiency of electrochemical chloride removal from concrete, ACI Mater. J. 103 (2006) 243–250.
[29] N.M. Ihekwaba, B.B. Hope, C.M. Hansson, Structural shape effect on rehabilitation of vertical concrete structures by ECE technique, Cem. Concr. Res. 26 (1996) 165–175.
[30] W. Yeih, J.J. Chang, A study on the efficiency of electrochemical realkalisation of carbonated concrete, Constr. Build. Mater. 19 (7) (2005) 516–524.
[31] A.M. Neville, Properties of Concrete, fourth ed., Longman Group Limited, 1995.
[32] W. Morris, E.I. Moreno, A.A. Sagues, Practical evaluation of resistivity of concrete in test cylinders a Wenner array probe, Cem. Concr. Res. 26 (12) (1996) 1779–1787.